

1 TranSPHIRE: Automated and feedback-optimized on-the-fly 2 processing for cryo-EM

3 Markus Stabrin, Fabian Schoenfeld, Thorsten Wagner, Sabrina Pospich,

4 Christos Gatsogiannis, Stefan Raunser*

5 *Department of Structural Biochemistry, Max Planck Institute of Molecular Physiology,*

6 *Otto-Hahn-Straße 11, 44227 Dortmund, Germany.*

7 (*corresponding author: stefan.raunser@mpi-dortmund.mpg.de)

8

9 Abstract

10 Single particle electron cryomicroscopy (cryo-EM) requires full automation to allow
11 high-throughput structure determination which is especially important for drug
12 discovery research. Although several software packages exist where parts of the
13 cryo-EM pipeline are automated, a complete solution that offers reliable, quality-
14 optimized on-the-fly processing, resulting in a high-resolution three-dimensional
15 reconstruction does not exist. Here we present TranSPHIRE: A software package for
16 fully automated processing of cryo-EM data sets during data acquisition. TranSPHIRE
17 transfers data from the microscope, automatically applies the common pre-
18 processing steps, picks particles, performs 2D clustering, and 3D refinement parallel
19 to image recording. Importantly, TranSPHIRE introduces a machine learning-based
20 feedback loop to re-train its internally used picking model to adapt to any given data
21 set live during processing. This elegant approach enables TranSPHIRE to process data
22 more effectively, producing high-quality particle stacks. TranSPHIRE collects, and
23 displays all microscope settings and metrics generated by its individual tools, in order
24 to allow users to quickly evaluate data during acquisition. TranSPHIRE can run on a
25 single work station and also includes the automated processing of filaments.

26

27 **Introduction**

28 Single particle electron cryomicroscopy (cryo-EM) has successfully established itself
29 as a prime method to determine the three-dimensional structure of macromolecular
30 complexes at close to atomic resolution ^{1,2}. The technique has therefore the potential
31 to become a key tool for drug discovery research ³. However, single particle analysis
32 (SPA) studies still require large amounts of processing time, expert knowledge, and
33 computational resources. With the number of modern high-throughput microscopes
34 growing rapidly, there is an urgent demand for a robust, automated processing
35 pipeline that requires little to no user intervention. This need is felt especially in the
36 field of drug discovery ³.

37 In many cases, data sets that were recorded for several days and can include
38 10,000 to 20,000 movies turn out to be unusable for high-resolution structure
39 determination during subsequent data processing. It is therefore necessary for users
40 to obtain feedback on the quality of their data immediately during recording. This
41 enables them to decide whether or not to continue a session, adjust any of the
42 acquisition parameters at the microscope, and compare different grids. This can only
43 be achieved when processing the data in parallel to data acquisition. A fully
44 automated pipeline requires streamlined data transfer and automated pre-
45 processing and processing workflows, free of any user bias.

46 Although several software packages partially address these issues ⁴⁻¹⁰, a
47 complete solution that offers reliable, quality-optimized and flexible on-the-fly
48 processing during data acquisition resulting in a high-resolution 3D reconstruction
49 does not yet exist. CryoFLARE ⁴, for example, performs live analysis and processing
50 parallel to data acquisition, but only to the level of 2D classification and lacks the
51 ability to perform *ab initio* 3D reconstructions or high resolution refinements.
52 Similarly, Focus ⁸, Appion ¹⁰, and Warp ⁶ do not produce 2D class averages and 3D

53 reconstructions. The latter two are less flexible than other offerings by being
54 restricted to either collecting data with Leginon ¹¹ in case of Appion or exclusive
55 compatibility with Windows and Warp-native tools. All three software packages
56 concentrate on data acquisition and associated parameters but not on the
57 optimization of data processing which is an important prerequisite for automated
58 structure determination. The non-interactive data pre-processing in Relion-3 ⁵ offers,
59 similar to Focus ⁸, some flexibility in terms of tool integration, but hinders the
60 implementation of more complicated cryo-EM processing by making advanced
61 parameters only accessible via manual scripting, rather than its GUI. Both Relionit ⁵
62 and Scipion ⁷ share the same accessibility issue of quality metrics, where no values
63 are automatically plotted and updated during processing. Instead, the user has to
64 step in and trigger the compilation of a log-file that contains a mix of metrics for all
65 processed data; any specific values of an individual micrograph have to be found
66 manually. This makes assessment problematic, especially for beginners in the field.

67 Here we present TranSPHIRE, a fully automated pipeline for on-the-fly
68 processing of cryo-EM data. It combines deep learning tools with a novel, feedback-
69 driven approach to re-train the integrated crYOLO particle picker ¹² during ongoing
70 pre-processing. This allows TranSPHIRE to perform GPU accelerated 2D classification
71 to provide high-quality 2D class averages and, subsequently, 3D reconstructions from
72 clean data. This gives experimentalists the means to quickly evaluate both the quality
73 of their data sets as well as their chosen microscope settings during data acquisition.
74 A combination of new and improved tools allows TranSPHIRE to provide users with
75 the strongest early results in the shortest amount of time, without the need to
76 outsource the computational load to a computer cluster, or the need for user
77 intervention. Importantly, it allows users to perform automated high-throughput on-
78 the-fly screenings for different buffer conditions or ligands of interest as well as to

79 fine-tune the workflow for the respective target-protein and perform digital
80 purification during image acquisition.

81

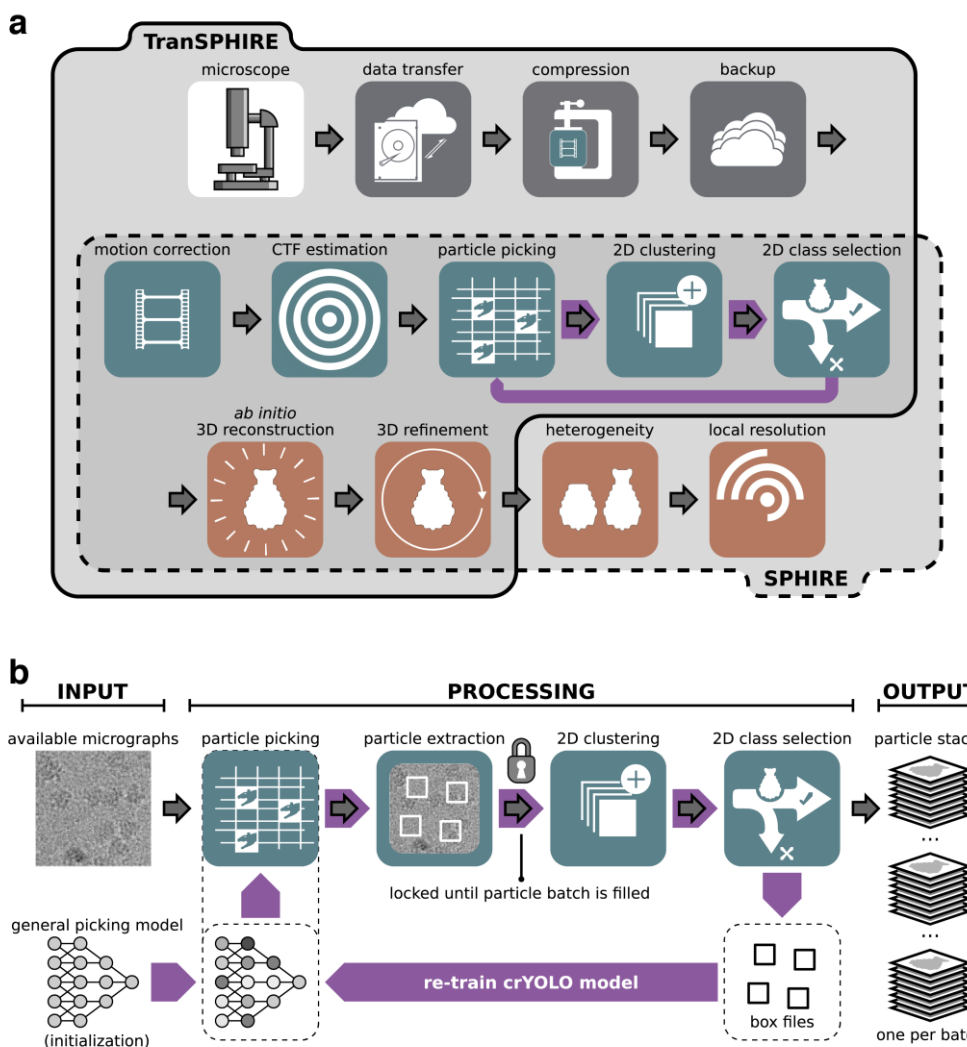
82 **Results**

83 **General setup, functionality and layout of TranSPHIRE**

84 TranSPHIRE is an automated pipeline for processing cryo-EM data sets (Figure 1). It is
85 developed in Python 3 to run on Linux, and is available online for free. TranSPHIRE
86 performs parallelized data transfer and flexibly integrates a range of commonly used
87 pre-processing tools, as well as the advanced processing tools of the SPHIRE package
88¹³. Using these tools, TranSPHIRE implements a fully automated pipeline to process
89 cryo-EM data on-the-fly during data acquisition. TranSPHIRE is designed to allow
90 users to make the best use of their available resources by prioritizing data analysis,
91 presenting early results, and using machine learning tools to identify and process
92 only those parts of the data that contribute to high quality results.

93 TranSPHIRE is controlled via an easy-to-use GUI that allows users to set up a
94 session, and choose and configure the desired tools to use (Supplementary Figure 1).
95 For pre-processing, the TranSPHIRE pipeline integrates MotionCor2¹⁴ and Unblur¹⁵
96 for beam induced motion correction with dose weighting; as well as CTFFIND4¹⁶,
97 CTER¹⁷, and GCTF¹⁸ for CTF estimation. This modularized integration is entirely
98 parameterized, allowing experimentalists to both choose their preferred tools as well
99 as configure them as needed – all without leaving the TranSPHIRE GUI. Available
100 parameters are sorted by level of usage (“main”, “advanced”, and “rare”) to highlight
101 and help identify the most commonly adjusted parameters for each tool.

102 During the session, TranSPHIRE automatically parallelizes the batch-wise
103 processing of incoming micrographs, outsources computationally expensive steps to



105 **Figure 1. The TranSPHIRE pipeline and the SPHIRE backend. (a) Upper register (solid**
106 **line):** Overview of the integrated TranSPHIRE pipeline and all automated processing
107 steps. The pipeline includes file management tasks, i.e., parallelized data transfer, file
108 compression, and file backup (grey); 2D processing, i.e., motion correction, CTF
109 estimation, particle picking, 2D clustering, and 2D class selection (turquoise); and 3D
110 processing, i.e., ab initio 3D reconstruction and 3D refinement (red). Additionally, the
111 pipeline includes an automated feedback loop optimization to adapt picking to the
112 current data set during runtime (purple). **Lower register (dotted line):** The SPHIRE
113 software package forms the backend for TranSPHIRE and offers the tools used for 2D
114 and 3D processing. SPHIRE includes additional tools for advanced processing, such as
115 heterogeneity analysis and local resolution determination. **(b)** The TranSPHIRE
116 feedback loop. Grey arrows indicate the flow of data processing. Red arrows indicate
117 the flow of the feedback loop. **Left (input):** Micrographs are initially picked using the
118 crYOLO general model. **Center (processing):** Particles are picked and extracted. Once

119 *a pre-defined number of particles have been accumulated, the pipeline performs 2D*
120 *classification; the resulting 2D class averages are labeled as either "good" or "bad" by*
121 *Cinderella. Class labels and crYOLO box files are then used to re-train crYOLO and*
122 *adapt its internal model to the processed data. In the next feedback round this*
123 *updated model is used to re-pick the data. **Right (output):** After five feedback rounds,*
124 *the complete data set is picked with the final optimized picking model and 2D*
125 *classified in batches. For every batch a particles stack of "good" particles is created*
126 *and available for 3D processing.*

127

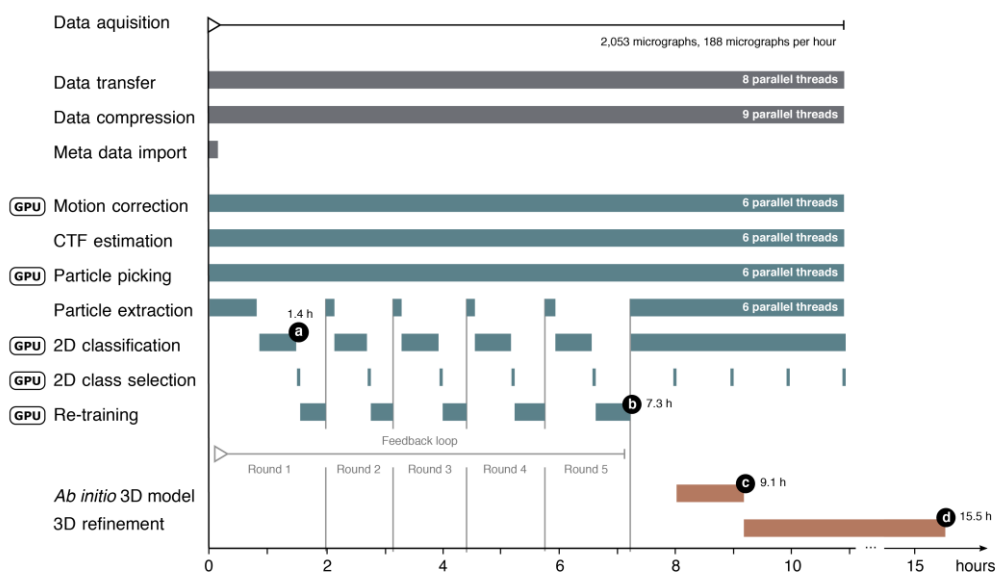
128 available GPUs, and produces preliminary 2D class averages and 3D reconstructions
129 based on the most recently processed batch of data (Figure 2, Supplementary Figure
130 2). Through the optimal distribution of processes, TranSPHIRE runs on-the-fly for a
131 wide range of data acquisition settings using a single workstation (Supplementary
132 Figure 3; see Methods for details about hardware). Moreover, TranSPHIRE can catch-
133 up with the speed of the acquisition after the initial delay due to the feedback loop
134 (see below) for routinely used data acquisition schemes (Figure 3c). Thus, initial 2D
135 class averages and 3D reconstructions are available within a few hours after starting
136 the data collection (Figure 2, Supplementary Figure 3).

137 Throughout the processing, TranSPHIRE collects all data quality metrics
138 produced by its individual tools, links them with the relevant micrographs where
139 appropriate, and presents them front and center in its GUI (Supplementary Figure 1).

140 Optionally, notifications for early milestones such as 2D class averages and
141 preliminary 3D maps, can also be sent via email. These features enable
142 experimentalists to both identify and address any issues as soon as they surface
143 during data acquisition, without requiring constant user supervision. Additionally, all
144 results produced by the integrated tools during processing are also copied in parallel
145 to the pre-defined workstation and backup locations (Supplementary Figure 2). To
146 support interoperability with existing packages, all pre-processing steps until particle

147 picking support the file formats used in both SPHIRE and RELION; for later processing
148 steps utilities are included to convert SPHIRE files into RELION .star.
149

150



151 **Figure 2. Timeline of the TranSPHIRE pipeline.** Timeline depicting the parallel
152 execution of the processes of the TranSPHIRE pipeline. Timings are based on a *Tc*
153 *holotoxin* data set consisting of 2,053 micrographs, each containing 36 particles on
154 average, collected at a speed of 188 micrographs per hour (K2 super-resolution, 40
155 frames). TranSPHIRE ran on-the-fly up to the creation of an *ab initio* 3D
156 reconstruction using default settings. Important milestones are denoted in black: (a)
157 first 2D class averages produced after 1.4h; (b) end of the feedback loop after 7.3h;
158 (c) *ab initio* 3D reconstruction after 9.1h; and (d) final 3D reconstruction of the first
159 batch of particles after 15.5h.

160

161 Transfer and pre-processing

162 Once a session starts, TranSPHIRE automatically detects and transfers new
163 micrographs from the camera computer of the microscope (Figure 1, Supplementary
164 Figure 2). These data are moved in parallel to several, user-specified locations e.g. a
165 work station or cluster for processing, and a backup storage server. In case of the
166 latter, TranSPHIRE also automatically compresses the data to preserve storage space.
167 Copy locations may also include additional spaces such as transportable hard discs. If

168 desired, TranSPHIRE further renames files, and deletes images from the camera
169 workstation in order to free up more space to enable continuous data collection. It
170 also extracts meta data such as acquisition time, grid square, hole number and
171 coordinates, spot scan, and phase plate position from .xml files provided by EPU or
172 .gtg files provided by Latitude S.

173 During the ongoing data transfer, any data that has already been copied is
174 pre-processed in parallel (Figure 2, Supplementary Figure 2). During setup, users can
175 choose to perform motion correction using either MotionCor2¹⁴ or Unblur¹⁵. While
176 motion correction is performed, TranSPHIRE presents all relevant metrics, such as the
177 average shift per frame, or the overall shift per micrograph (Supplementary Figure 1).
178 For CTF estimation, users can set up TranSPHIRE to use either CTFFIND4¹⁶, CTER¹⁷,
179 and GCTF¹⁸. Depending on whether or not CTF estimation on movies is activated in
180 TranSPHIRE, CTF estimation is performed in parallel to motion correction
181 (Supplementary Figure 2). The metrics extracted and displayed by TranSPHIRE
182 include defocus, astigmatism, and the resolution limit (Supplementary Figure 1).
183 Combined with the information gathered during motion correction, these values
184 allow experimentalists to assess the performance and alignment of the microscope
185 during acquisition, and adjust any thresholds to automatically discard low quality
186 micrographs as necessary.

187 For particle picking the TranSPHIRE pipeline integrates crYOLO¹², our state of
188 the art deep learning particle picker. During picking, TranSPHIRE displays the particles
189 picked per micrograph, which allows users to assess the picking performance and
190 overall sample quality (Supplementary Figure 1).

191 Once a fixed threshold of picked particles is reached (Supplementary Figure
192 4; also see Methods), TranSPHIRE launches 2D classification using a GPU accelerated
193 version of ISAC2¹⁹ (Figure 1). ISAC2 limits the number of class members to spread the

194 given particles across multiple classes which prevents individual classes from growing
195 too large. This results in sharp, equal-sized, and reproducible classes that contain all
196 possible orientations exceeding the minimum class size. They enable
197 experimentalists to reliably assess particle orientations and overall quality, and help
198 to identify possible issues such as preferred orientations or heterogeneity.

199 The 2D class averages are then sorted by Cinderella²⁰, our integrated deep
200 learning tool for 2D class selection. Cinderella labels the given 2D classes as either
201 “good” or “bad” and determines which class averages and, thereby, particles are
202 used for further processing. This results in an automatic cleaning of the data and
203 allows TranSPHIRE to process only the relevant subset of a given data set, thereby
204 dramatically lowering the amount of data processed by the computationally
205 expensive steps of 3D reconstruction and refinement.

206

207 **Optimizing particle picking using a machine learning-fueled feedback loop**

208 For any cryo-EM pipeline the ability to reliably perform high quality picking
209 irrespective of the data at hand is essential. This poses a challenge when processing
210 is to be automated, as this immediately excludes any user intervention such as
211 manual inspection of the picking results. The latter is especially relevant if a sample is
212 unknown to the picking procedure, or is otherwise difficult to process, e.g. due to
213 contamination or interfering conformational states – issues that usually need to be
214 identified by a qualified expert before processing can continue.

215 TranSPHIRE solves these issues by introducing a machine learning based
216 feedback loop that repeatedly re-trains the fully integrated crYOLO¹² deep learning
217 particle picker during data acquisition to adapt picking to the given data set (Figure
218 1b). This enables crYOLO to specifically target those particles that end up in stable 2D
219 class averages, while, at the same time, learning to disregard particles that do not.

220 First, incoming motion corrected micrographs are forwarded to crYOLO for picking.
221 Once a batch of 20,000 picked particles has been accumulated, it is handed over to
222 our GPU accelerated version of the 2D classification algorithm ISAC2¹⁹
223 (Supplementary Figure 3). Here we determine which particles can be used to create
224 stable 2D class averages, and reject the particles that cannot be accounted for. The
225 newly produced 2D class averages are given to our deep learning tool Cinderella²⁰,
226 which labels each class average as either “good” or “bad”. At this point, the particles
227 of the “good” classes are used to re-train crYOLO and update its internal model.
228 Specifically, we randomly select a maximum of 50 micrographs that contain particles
229 that ended up in the “good” classes for the re-training (for details see Methods).
230 Once the training and thus the first feedback round has completed, processing re-
231 starts using the optimized picking model (Figure 1b).

232 The TranSPHIRE feedback loop iterates five times, which has proven sufficient
233 to achieve convergence in our experiments, and afterwards is not repeated for the
234 remainder of the data acquisition. Re-training crYOLO¹² to become increasingly more
235 proficient at targeting particles that end up in “good” classes has the additional
236 benefit of trimming down the overall size of the data set. Though the pre-processing
237 of cryo-EM data is already time consuming, the following 3D refinement requires
238 even more computational power. While it is usually customary to process as much
239 data as possible, the computational cost of 3D refinement usually does not scale
240 linearly, and such an approach will not be sustainable in the near future. This is
241 further exacerbated by the fact that image acquisition speeds and sizes of data sets
242 are both growing rapidly. Because of this, the aim should be to process as little data
243 as necessary, without harming the quality of the final reconstruction. Fortunately, it
244 is known that cryo-EM data sets contain a large amount of unusable data that can be
245 safely discarded – if we have a way to reliably ensure that we keep those data that

246 we are actually interested in. The TranSPHIRE feedback loop offers this functionality
247 and provides quality in quantity.

248

249 ***Ab initio* 3D model reconstruction and 3D refinement**

250 To compute a 3D reconstruction, the particles included in all classes labeled “good”
251 by Cinderella are extracted and form a clean, high-resolution particle stack. If there is
252 no initial 3D reference provided to TranSPHIRE, the pipeline waits until at least 200
253 (by default) “good” classes have been accumulated. The respective 2D class averages
254 are then used to create a reproducible, *ab initio* 3D reconstruction using SPHIRE
255 RVIPER^{13,21} (Figure 1). This provides a first view of the structure of the target protein
256 and a first impression of the conformational state.

257 The initial 3D reference is then used by TranSPHIRE to initialize the 3D
258 refinement using SPHIRE MERIDIEN (Figure 2). While the initial map is computed only
259 once, a new 3D refinement is started every time another set of 40,000 (by default)
260 “good” particles has been accumulated.

261 Note that in contrast to SPHIRE RVIPER, which only uses the first 2D class
262 averages, SPHIRE MERIDIEN uses all particles subsumed by the last batch of “good”
263 particles. The fully automated creation of an initial 3D map and continuous
264 production of a series of refined reconstructions based on that latest data enables
265 TranSPHIRE to present high-resolution structures already during data acquisition.

266 This enables for a more detailed, on-the-fly evaluation by the user, such as
267 analyzing the conformational state and/or confirming whether and where a ligand is
268 bound. By providing a series of reconstructions – one for every batch, TranSPHIRE
269 also offers a time-resolution of the data set, enabling experimentalists to gauge the
270 quality of their data over time throughout data acquisition.

271 With the following three experiments we illustrate the capabilities of
272 TranSPHIRE to automatically adapt to unknown data, make use of prior knowledge to
273 selectively target the conformational subpopulation within a sample and process
274 filamentous data.

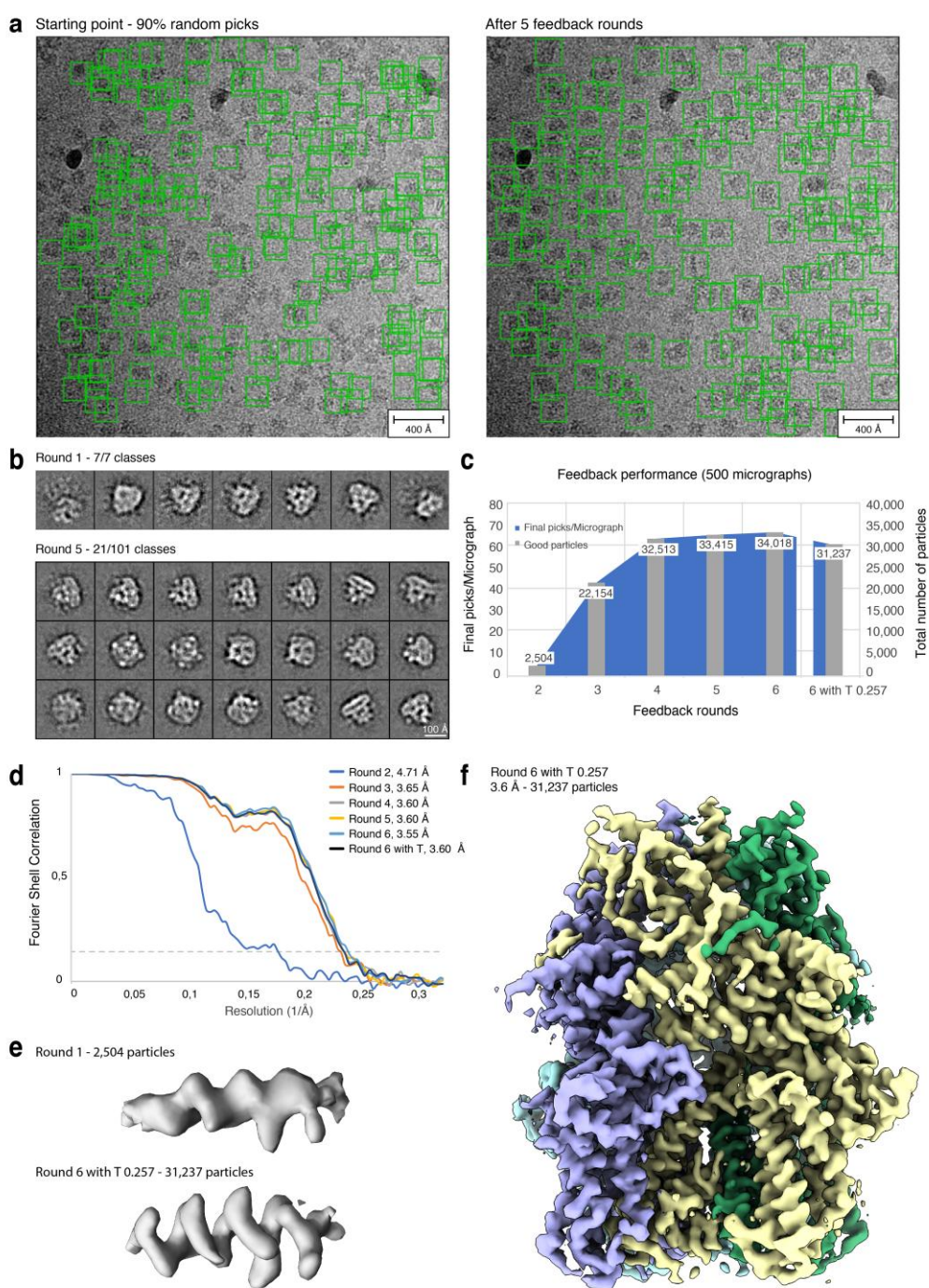
275

276 **Learning to pick an initially unknown membrane channel without user intervention**

277 Similar to crYOLO, many modern particle picking programs are based on machine
278 learning, where an internal model is trained to recognize particles within
279 micrographs^{6,22,23}. While this method features an inherent capacity to generalize to
280 unseen data sets, this ability is limited. Therefore, reliable picking can usually not be
281 guaranteed out of the box when samples differ too much from the original training
282 data of the network. Samples might also be of unusually low contrast, or an unknown
283 form of contamination is encountered. While such issues can be overcome by adding
284 the problematic data to the training set, this requires manual user intervention on
285 multiple levels. First, the insufficient picking capability has to be detected; second, an
286 experienced experimentalist has to pick a small amount of training data by hand; and
287 third, the network has to be re-trained manually.

288 The TranSPHIRE feedback loop resolves this issue and entirely foregoes the
289 need for user intervention even when facing data that is either unknown to the
290 picking model or yields insufficient picking results for any other reason. To
291 demonstrate this ability, we processed a data set of the TRPC4 membrane protein
292 channel with the TranSPHIRE feedback loop using a picking model without any prior
293 knowledge of this protein (Figure 3). Specifically, to ensure the sample was unknown
294 to crYOLO at the start of the feedback loop, we removed all four TRP channel data
295 sets normally included in the training data of the crYOLO general model. Additionally,
296 in order to simulate a bad generalization of crYOLO we randomized 90% of all picks in

297



298

299

300 **Figure 3. Processing the TRPC4 membrane channel using a deliberately hampered**
301 **picking model. (a)** To simulate low quality picking, only 10% of the initial crYOLO
302 picks were used while the remaining 90% were re-positioned randomly (**left**). After
303 the feedback loop crYOLO reliably picks the TRPC4 particles (**right**). **(b)** Total amount
304 of 2D class averages produced in the first iteration of the feedback loop (**top**) and 21
305 representative averages produced in the final iteration of the feedback loop (**bottom**).
306 **(c)** Progression of the number of particles labeled “good” when applying the
intermediate picking models of the feedback loop to a fixed subset of 500

307 *micrographs. The curve flattens out in the final iterations, indicating the convergence*
308 *of the feedback loop optimization. (d) Fourier shell correlation (FSC) curves of the*
309 *individual 3D reconstructions computed from particles labeled “good” (also see c). (e)*
310 *Representative alpha-helix (amino acids 600-615) illustrating the improvement of the*
311 *density when using the final (bottom) compared to the initial (top) picking model. (f)*
312 *3D reconstruction of TRPC4 computed from 500 micrographs using the optimized*
313 *picking model.*

314

315 the first iteration of the feedback loop (Figure 3a). This was done by replacing 90% of
316 the particle boxes determined by crYOLO with randomly positioned boxes within the
317 same micrographs. In combination, these measures ensured that the initial picking
318 results were almost entirely unusable and successful re-training had to take place in
319 order to enable further processing of the data.

320 Despite the bad starting point, by the final feedback loop iteration the
321 repeatedly re-trained model has successfully learned to pick the previously unknown
322 TRPC4 particles resulting in high-resolution 2D class averages (Figure 3a, b). An
323 evaluation of the performance of the feedback loop on a fixed subset of 500
324 micrographs (see Methods for details), illustrates that the number of “good” particles
325 increases sharply within the early iterations of the feedback loop from an initial 25%
326 of particles to a stable value of ~ 50%, (Table 1, Figure 3c) and a final resolution of 3.6
327 Å (FSC=0.143). This increased ability to identify a greater number of usable particles
328 on the same subset of micrographs is also reflected in the map quality and achieved
329 resolution when using the intermediate crYOLO models produced during the
330 individual feedback rounds to process the fixed set of 500 micrographs (Figure 3d-f).

331 This experiment furthermore demonstrates the ability of crYOLO to adapt to
332 unknown data even if only sparse training data is available. In the initial round of the
333 feedback loop a mere 5 particles per micrograph ended up in “good” classes on

334 average – and, consequently, are all that was available to re-train the picking model
335 (Table 1).

<i>Feedback round</i>	<i>Good classes</i>	<i>Good particles</i>	<i>Picks/Mic</i>	<i>Good picks/Mic</i>	<i>Resolution</i>	<i>Relative good picks</i>
2	28	2,504	20	5	4.71	0.25
3	236	22,154	104	44	3.65	0.43
4	349	32,513	132	65	3.60	0.49
5	355	33,415	152	67	3.60	0.44
6	361	34,018	147	68	3.55	0.46
6 + T 0.257	331	31,237	114	62	3.6	0.55

336
337 **Table 1. TRPC4 feedback loop statistics.** For every feedback round as well as the final
338 run after optimization of the picking threshold (6 + T x.xx) the number of classes
339 labeled “good” by Cinderella; the number of particles included in these classes; the
340 total number and the number of good particles picked per micrograph; the final
341 resolution of the 3D reconstruction; and the relative amount of good particles are
342 listed for the TRPC4 data (500 micrographs).

343
344 In summary, the TranSPHIRE feedback loop is able to automatically optimize
345 the internally used picking model and provide reliable, high quality picking results
346 even when processing challenging samples that initially are barely recognized by the
347 model. We have shown that in such a case, after five feedback rounds, crYOLO is able
348 to pick the TRPC4 membrane protein to completion, without requiring the user to
349 continuously monitor, let alone disrupt the ongoing data processing. The feedback
350 loop optimization is fully integrated into the TranSPHIRE pipeline and works entirely
351 automated out of the box. Its capabilities extend to difficult data sets such as
352 membrane proteins, and enable advanced processing methods, such as targeting
353 specific conformational states, or processing filamentous data sets, as demonstrated
354 in the following.

355

356

357 **Selectively targeting a conformational state in a mixed sample using prior
358 knowledge**

359 A basic assumption of most algorithms currently used to process cryo-EM data is that
360 all particles in a data set are projections of the same structure, hidden behind a
361 curtain of noise. In reality, however, cryo-EM samples are often more complex, and
362 can contain multiple conformational states of the target structure, impurities, and
363 aggregates. Filtering such unwanted data and selectively targeting only a subset of
364 the structures found within a sample is one of the fundamental issues in cryo-EM,
365 and often requires significant efforts to address and resolve.

366 The TranSPHIRE feedback loop offers a straightforward solution to this issue by
367 allowing the injection of additional knowledge into the pipeline, either before or
368 during runtime. This enables users to incorporate and make use of information that is
369 already available, as well as information that was just produced during acquisition.

370 Specifically, a set of 2D class averages of the target structure can be used to train
371 Cinderella²⁰ to only recognize these averages as representatives of “good” classes,
372 and, consequently, everything else as “bad.” If such averages are available
373 beforehand, Cinderella can be pre-trained; otherwise the feedback loop can be
374 paused once the first set of 2D class averages are produced in the TranSPHIRE
375 pipeline and continued after manual re-training of Cinderella. This additional training
376 step to embed additional knowledge into the TranSPHIRE pipeline enables us to steer
377 the re-training of the picking model during the feedback loop iterations. More
378 precisely, particles that end up in sharp classes depicting a different particle, a
379 subcomplex, and/or the target protein in the wrong conformational state (for
380 example) will now also be labeled as “bad” by Cinderella, despite their high quality.

381 During the feedback loop, crYOLO will thus be taught to only focus on particles that

382 end up in quality classes depicting the wanted particle or state, while, at the same
383 time, reject anything else, including sharp classes from an unwanted subpopulation.
384 To demonstrate the capability of the TranSPHIRE feedback loop to use prior
385 knowledge and target a pre-selected conformation, we processed a sample of the Tc
386 holotoxin that contained particles in two conformational states, namely the pre-pore
387 and pore state (Figure 4a). Of these, we only targeted the pore state, which is
388 significantly more difficult to find as it only accounts for ~ 19% of the particles within
389 the data set (Table 2, Figure 4b). Cinderella was trained with 318 examples of “good”
390 classes (side-views of the pore state) and 664 examples of “bad” classes (views of the
391 pre-pore state and contamination). During the feedback loop crYOLO was then re-
392 trained with only those particle picks that ended up in “good” classes showing views
393 of the pore state.

Feedback round	Good classes	Good particles	Picks/Mic	Good picks/Mic	Resolution	Relative good picks
1	130	12,595	130	25	4.28	0.19
2	145	10,406	100	21	4.24	0.21
3	151	14,534	74	29	4.36	0.40
4	146	14,081	71	28	4.28	0.40
5	155	14,935	68	27	4.28	0.40
6	140	13,566	69	27	4.24	0.39
6 + T 0.194	145	13,954	55	28	4.24	0.50

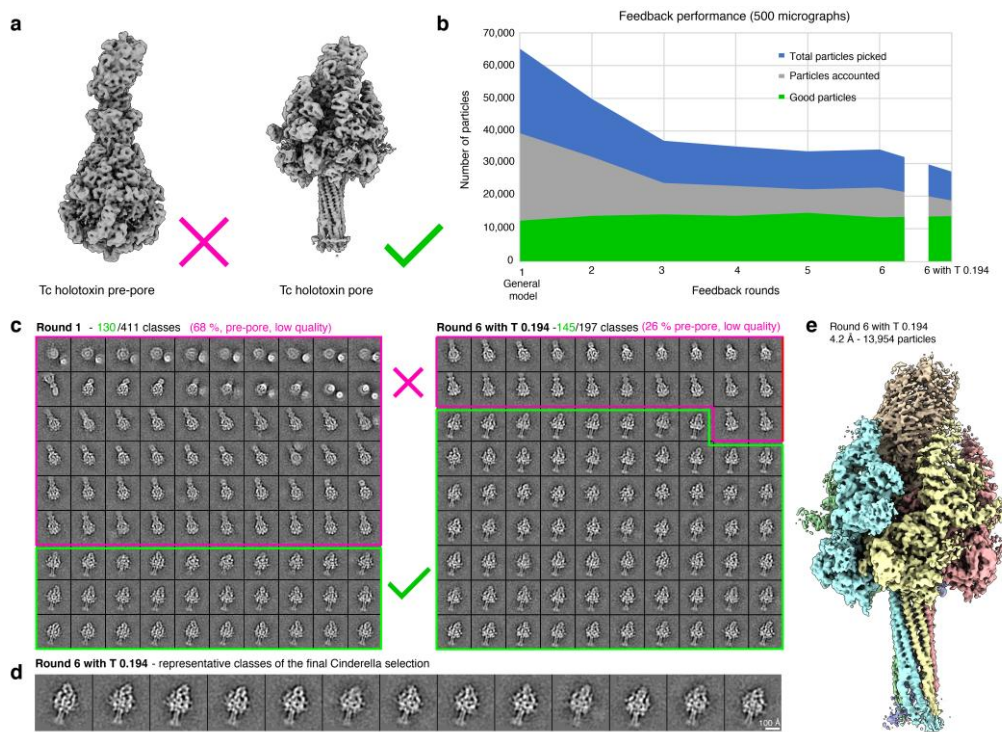
394
395 **Table 2. Tc holotoxin feedback loop statistics.** For every feedback round as well as
396 the final run after optimization of the picking threshold (6 + T x.xx) the number of
397 classes labeled “good” by Cinderella; the number of particles included in these
398 classes; the total number and the number of good particles picked per micrograph;
399 the final resolution of the 3D reconstruction; and the relative amount of good
400 particles are listed for the Tc Holotoxin data (500 micrographs).

401
402 To evaluate the performance of the feedback loop we used the intermediate
403 picking models produced during the individual feedback rounds to separately process
404 a fixed set of 500 micrographs once the feedback loop had finished (see Methods for

405 details). We observed a steady decrease of particles representing the pre-pore state
406 – that we are not interested in – together with an initial rise and then level amount of
407 pore state picks (Figure 4b, Table 2). While initially only 19% of the particles
408 resembled the pore state, slightly more than 50% of all picks ended up in 2D class
409 averages depicting our targeted conformation when using the final optimized picking
410 model (Figure 4c-d). As in the previous experiment, the percentage of relative good
411 picks per micrograph steadily increases. Notably, this happens while neither the
412 number of good classes, nor the number of good particles seem to follow suit (Table
413 2). This means that our re-training efforts are working as intended: Over the course
414 of the feedback loop, crYOLO learns to discard quality class averages of the pre-pore
415 state that we are not interested in and instead focus on picking the less common
416 pore state. Consequently, the amount of picked particles changes slowly, while, at
417 the same time, the relative amount of “good” particle picks steadily increases,
418 resulting in a 4.2 Å (FSC=0.143) 3D reconstruction of the pore state from no more
419 than 500 micrographs (Figure 4e).

420 Taken together, these results illustrate how additional knowledge can be
421 used to pre-train Cinderella, allowing TranSPHIRE to steer the re-training of the
422 picking model during the feedback loop and to target a known subpopulation within
423 the data. Using a picking model optimized for a specific conformation offers a two-
424 fold advantage. First, reconstruction efforts will be more effective, as we gain more
425 particles of the subpopulation that we are interested in. Second, reconstruction
426 efforts will be more efficient, as the rejection of particles that end up in “bad” classes
427 significantly shrinks the overall size of the data set. In our example, we reduce the
428 number of picked particles from an initial total of 67,117 to a set of only 27,646
429 particles, without reducing the achieved resolution or the number of pore state
430 particles that we are interested in (Figure 4b). Any follow-up computations, such as

431 costly 3D reconstructions, benefit greatly from such a reduction in data set size as it
432 results in a much more efficient use of the available computational resources.
433



434
435 **Figure 4. Using prior knowledge to extract a pre-selected conformational state. (a)**
436 The processed data set contains the Tc holotoxin in both the pre-pore state (**left**) and
437 the more rare pore state (**right**). In this experiment we specifically target the pore
438 state. **(b)** Progression of the number of picked particles (blue), those accounted during
439 2D classification (grey) and particles labeled “good” i.e. representing the pore state
440 (green) when applying the intermediate picking models of the feedback loop to a
441 fixed subset of 500 micrographs. Initial picking is dominated by pre-pore state
442 particles. This overhead is reduced with each iteration, while the amount of picked
443 pore state particle remains stable. **(c)** Representative 2D class averages depicting the
444 decrease of unwanted classes (pore state or low quality; marked red) from an initial
445 68% in the first feedback round (**left**) to 26% after the last feedback round (**right**). **(d)**
446 Representative 2D class averages depicting the pore state as selected by Cinderella in
447 the final iteration of the feedback loop. **(e)** 3D reconstruction of the Tc holotoxin pore
448 state computed from 500 micrographs using the final optimized picking model.

449

450

451 **Using TranSPHIRE to automatically process filamentous proteins**

452 Filamentous proteins such as the actomyosin complex are notoriously difficult to
453 process. This is because their structure is by definition not limited to a single element
454 but rather forms a continuous strand that both enters and exits the enclosing frame
455 of any picked particle image. Consequently, filamentous proteins are traced, rather
456 than picked, and overlapping segments have to be identified along each filament,
457 while filament crossings and contamination need to be avoided. In addition,
458 filamentous projections share a similar overall geometry which increases the
459 correlation between any two particles and interferes with alignment attempts during
460 2D classification. While there are several programs available that implement manual
461 filament processing^{13,24-27}, until now there has not yet been any cryo-EM software
462 package that offers the automated processing of filamentous data sets.

463 With TranSPHIRE we introduce a comprehensive software package for cryo-
464 EM that includes the ability to automatically process filamentous proteins utilizing
465 methods of the SPHIRE package¹³. While the actual processing is fully automated,
466 some preparation is still needed when using the TranSPHIRE pipeline to process
467 filaments. Specifically, crYOLO needs to be trained to pick filaments²⁸, as these look
468 fundamentally different from the single particle complexes known to its default
469 general model. Additionally, Cinderella²⁰ also needs to be trained with 2D class
470 averages of the filament in question. If such class averages are not available initially,
471 the feedback loop can be halted for re-training Cinderella as soon as TranSPHIRE has
472 produced them. Once the models for the deep learning decision makers of the
473 pipeline are trained on the specific filamentous data, TranSPHIRE and its integrated
474 feedback loop are ready to automatically process the respective filamentous data
475 sets.

476 As an example of processing initially unknown filamentous data, we chose an
477 actomyosin complex. To further demonstrate the ability of the feedback loop to
478 adjust the picking to a specific filamentous protein complex, we trained crYOLO with
479 multiple data sets of F-actin, which looks substantially different than the actomyosin
480 complex (Figure 5a). Thereby, crYOLO learns to trace filaments, but does not readily
481 recognize actomyosin filaments resulting in a weak initial picking performance
482 (Figure 5b-c).

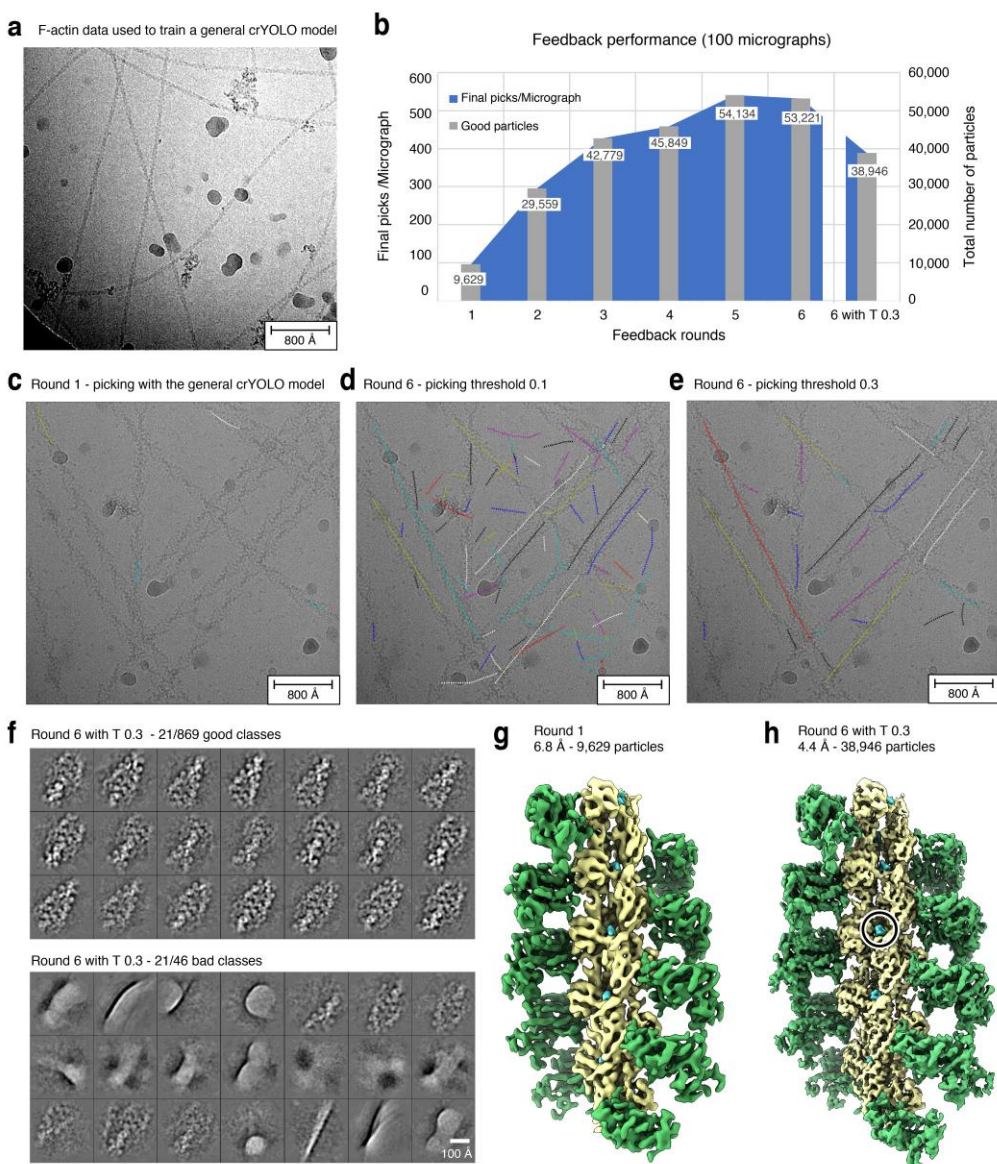
483 As soon as the first 2D class averages became available, the feedback loop
484 was halted and a new Cinderella model was trained manually. Afterwards the
485 feedback loop continued through its default five iterations, automatically teaching
486 crYOLO to identify projections of the actomyosin complex. To evaluate the
487 performance of the feedback loop we separately processed a fixed set of 100
488 micrographs using the intermediate picking models produced during the individual
489 feedback iterations (Figure 5, Table 3, see Methods for details).

Feedback round	Good classes	Good particles	Picks/Mic	Good picks/Mic	Resolution	Relative good picks
1	211	9,629	143	96	7.63	0.67
2	659	29,559	358	296	4.48	0.83
3	936	42,779	552	428	4.37	0.77
4	1,016	45,849	639	458	4.54	0.72
5	1,203	54,134	1,098	541	4.32	0.49
6	1,174	53,221	1,073	532	4.72	0.50
6 + T 0.3	869	38,946	515	389	4.54	0.76

490

491 **Table 3. Actomyosin complex feedback loop statistics.** For every feedback round as
492 well as the final run after optimization of the picking threshold (6 + T x.xx) the number
493 of classes labeled “good” by Cinderella; the number of particles included in these
494 classes; the total number and the number of good particles picked per micrograph;
495 the final resolution of the 3D reconstruction; and the relative amount of good
496 particles are listed for the actomyosin complex data (100 micrographs).

497



498

499 **Figure 5. Ligand identification within an actomyosin complex. (a)** Representative
500 **micrograph of the F-actin data used to train crYOLO. (b)** Progression of the number of
501 "good" particles per micrograph (blue) and in total (grey) when applying the
502 intermediate picking models of the feedback loop to a fixed subset of 100
503 micrographs. The dipping curve at the end indicates the desired loss of low-quality
504 picks that are excluded when a higher picking threshold (0.3) is used. **(c)** Representative
505 micrograph of the actomyosin complex highlighting the weak initial
506 picking results when using the crYOLO model trained on F-actin data (see **a**). **(d)**
507 Particle picking performance on the same micrograph using the final picking model.
508 While filaments are now traced much more effectively, the model also picks
509 unwanted filament crossings and contamination. **(e)** Increasing the picking threshold
510 from 0.1 to the default value of 0.3 minimizes the amount of false positive picks, while

511 *maintaining the desired filament traces. (f) Representative 2D class averages labeled*
512 *“good” (top) and “bad” (bottom) by Cinderella based on 100 micrographs and using*
513 *the final model for picking. (g) 3D reconstruction of the actomyosin complex*
514 *computed from 100 micrographs using the initial picking model. (h) 3D reconstruction*
515 *computed from the same 100 micrographs using the final optimized picking model.*
516 *The resolution is sufficient to verify the binding of a ligand (circled).*

517

518 Initially a low confidence threshold of 0.1 (default) was used for picking in
519 order to gather enough training data (Figure 5c, d). However, the amount of picked
520 particles and the confidence in the picks increased throughout the feedback loop
521 (Figure 5b, c). Thus, the picking threshold was adjusted to the default value of 0.3
522 after the feedback in order to exclude low confidence picks of contamination and
523 filament crossings (Figure 5b, d-e). Thereby, the number of relative good particles
524 could be increased from 50% to 76% (Table 3) resulting in few classes labeled “bad”
525 (Figure 5f). The improvement is also visible when comparing the initial and final 3D
526 reconstruction computed from the same set of 100 micrographs (Figure 5g-h).
527 Particularly, the final reconstruction of 4.4 Å (FSC=0.143) is sufficient to identify a
528 small molecule bound to the filament, highlighting how TranSPHIRE can simplify
529 ligand screenings.

530 Using the feedback loop, TranSPHIRE offers the first cryo-EM software
531 package that is able to automatically process filamentous data, even if the precise
532 shape of a specific filament is initially unknown to the pipeline. Moreover,
533 TranSPHIRE now enables experimentalists to produce an early 3D reconstruction with
534 a resolution sufficient to identify bound ligands and determine whether or not their
535 data is likely to yield a high resolution reconstruction – all within the time frame of
536 hours and while their data is still being collected at the microscope (Figure 2,
537 Supplementary Figure 3). The automated processing greatly simplifies the processing

538 of filamentous samples in general and, most importantly, facilitates the fast
539 determination of multiple structures of one filament decorated with different
540 accessory proteins or bound to ligands.

541

542 **4 Discussion**

543 In this paper we present the streamlined TranSPHIRE pipeline for automated,
544 feedback-driven processing of cryo-EM data. It fully automates data transfer, pre-
545 processing and the creation of a series of early reconstructions based on the most
546 recently processed data (Figure 1a). At the same time, TranSPHIRE prominently
547 displays all relevant data evaluation metrics, updated in real time (Supplementary
548 Figure 1), and offers the option to send email notifications when issues are
549 encountered or important milestones – such as the first 2D class averages, or an
550 initial 3D reconstruction – have been reached.

551 We also introduce the TranSPHIRE feedback loop (Figure 1b), a machine
552 learning-based method to optimize the internally used particle picking model and
553 adapt our native crYOLO picker to any data set, even while it is still being collected at
554 the microscope. This allows TranSPHIRE to adjust to never before seen data, as well
555 as to avoid any issues that a cryo-EM sample might include, such as unwanted
556 proteins, low contrast, and/or different kinds of contamination. The optimization of
557 the picking model performed by the feedback loop can further be guided by the
558 experimentalist in order to specifically select a subpopulation within the data, such as
559 a distinct conformational or oligomeric state.

560 We demonstrate these capabilities of TranSPHIRE and its new feedback loop
561 by performing three distinct experiments, each addressing a common issue in cryo-
562 EM: First, we processed the membrane protein TRPC4, after purposefully sabotaging
563 our particle picking to simulate processing a data set that is not only unknown, but

564 initially only barely provides enough useful picks for training. Nevertheless, the
565 TranSPHIRE feedback loop successfully taught crYOLO to identify and pick the sought-
566 after particles without any need for user intervention or expert knowledge input.
567 When the final picking model was then used to automatically compute a full
568 reconstruction, we reached a resolution of 3.6 Å (FSC=0.143), based on the data
569 extracted from no more than 500 micrographs (Figure 3).

570 Second, we processed a sample containing the Tc holotoxin in two different
571 conformational states: The common pre-pore state, and the significantly rarer pore
572 state that only accounts for about one fifth of the available particles. In this
573 experiment we injected prior knowledge about the pore state into the pipeline by
574 training Cinderella – our deep learning tool to reject unusable 2D class averages – to
575 only accept class averages of this state. This directed the re-training during the
576 feedback loop and taught crYOLO to focus on the rare pore state particles. As a
577 result, we obtained a picking model that was highly selective for only one
578 conformational state while rejecting not only low quality 2D class averages, but also
579 high quality 2D class averages if they displayed the Tc holotoxin in the
580 conformational state that we were not interested in (Figure 4). This produced a
581 particle stack that was not only populated with an increased number of “good”
582 particles, but also contained less particles overall, as unwanted particles were already
583 rejected during particle picking. The final reconstruction obtained a resolution of 4.2
584 Å (FSC=0.143). Such an optimized stack means that any follow-up computations only
585 have to deal with relevant data, allowing for a more efficient use of the available
586 computational resources.

587 Third, we processed a data set of an actomyosin complex to demonstrate
588 how the ability of TranSPHIRE to automatically process cryo-EM data also extends to
589 filamentous proteins. To adjust the pipeline to the processing of filaments, we re-

590 trained both crYOLO and Cinderella in order to teach them about the distinct visual
591 properties of filamentous particles and how to avoid any filament-exclusive pitfalls,
592 such as filament crossings. To specifically showcase the ability of the feedback loop
593 to deal with an initially unknown filament structure, we only taught crYOLO about F-
594 actin, which features a fundamentally different appearance than the actomyosin
595 complex. Cinderella was then only trained with the initial 2D class averages that
596 TranSPHIRE produced during the first iteration of the feedback loop. Despite the
597 initial picking model only knowing about F-actin, Cinderella was able to teach crYOLO
598 about the actomyosin complex and the final reconstruction reached a resolution of
599 4.4 Å (FSC=0.143), using the data extracted from merely 100 micrographs (Figure 5).

600 In summary, TranSPHIRE offers a fully automated pipeline that produces
601 highly optimized particle stacks that allow for more effective processing and more
602 efficient use of any available resources, both computational and human. Combined,
603 these features allow experimentalists to make the most of their limited time at the
604 microscope and to identify and address any issues as soon as they surface.
605 Furthermore, TranSPHIRE produces early reconstructions of proteins, even if initially
606 unknown, thereby enabling experimentalists to assess their data and identify the
607 conformational state of their protein or validate the binding of a ligand while their
608 data is still being collected. Hence, TranSPHIRE allows users to perform automated
609 high-throughput on-the-fly screenings for different buffer conditions or ligands of
610 interest.

611

612 **Methods**

613 **Hardware used to run TranSPHIRE**

614 By default, TranSPHIRE runs on a single machine, which can be combined with a
615 separate workstation or computer cluster to outsource computational power. For the

616 majority of the results presented in this manuscript, a single machine equipped with
617 two Intel(R) Xeon(R) Gold 6128 CPUs (3.40GHz), featuring 12 CPU cores each
618 (hyperthreading 24); 192 GB of RAM; and three GeForce RTX 1080 Ti GPUs was used.
619 Only computationally more expensive 3D reconstructions, both the initial *ab initio*
620 reconstruction and the 3D refinements (for details see below), were outsourced to
621 our local computer cluster. There, calculations were performed on two nodes; each
622 equipped with two Intel(R) Xeon(R) Gold 6134 CPUs (3.20GHz), featuring 32 CPU
623 cores in total and 384 GB of RAM.

624

625 **Software integrated into the TranSPHIRE pipeline**

626 TranSPHIRE is a free of charge, open-source software written in Python3, which is
627 available online (<https://github.com/MPI-Dortmund/transphire>).

628 Its fully-automated processing pipeline integrates several software packages
629 and is thereby highly flexible and adaptable. An initial integrity check and the
630 consecutive compression of every input stack to a LZW compressed tiff file is
631 performed using IMOD v4.9.8³⁰. Currently, TranSPHIRE supports several options for
632 motion correction (Unblur¹⁵ and MotionCor2¹⁴) and CTF estimation (CTFFIND¹⁶,
633 CTER¹⁷ and GCTF¹⁸). For all consecutive 2D and 3D processing steps, TranSPHIRE
634 utilizes functions of the SPHIRE¹³ package including the deep-learning particle picker
635 crYOLO¹², the 2D class selection tool Cinderella²⁰ and a new GPU accelerated version
636 of the reliable 2D classifier ISAC2¹⁹.

637 Results presented in this manuscript were generated with TranSPHIRE
638 v1.4.50 and SPHIRE v1.4. Specifically, the pipeline consisted of the following modules:
639 the CUDA 10.2.86 version of MotionCor2 v1.3.0¹⁴; CTFFIND v4.1.13 for CTF
640 estimation¹⁶; crYOLO v1.6 for particle picking¹²; SPHIRE sp_window.py for particle
641 extraction¹³; a GPU accelerated version (v1.0) of SPHIRE ISAC2¹⁹ for on-the-fly 2D

642 classification (will be published elsewhere); SPHIRE Cinderella v0.5 ²⁰ for 2D class
643 selection; SPHIRE sp_rviper.py ^{13,21} for *ab initio* reconstructions and finally SPHIRE
644 sp_meridien.py ¹³ or sp_meridien_alpha.py for the 3D refinement of single particles
645 or filaments, respectively.

646

647 **The automated processing pipeline within TranSPHIRE**

648 After preprocessing the data i.e. data transfer and compression, motion correction
649 and CTF estimation (also see Supplementary Figure 2), particles are automatically
650 picked using the deep learning, GPU-accelerated particle picker crYOLO ¹². By using
651 the general model, which was trained on 63 cryo-EM data sets, crYOLO is able to pick
652 previously unseen particles. During the feedback rounds a picking threshold of 0.1 is
653 used to facilitate the picking of distinct proteins and features. At the end of each
654 feedback iteration crYOLO is retrained on particles that contributed to classes labeled
655 “good” by Cinderella (see below and Figure 1b). When crYOLO is trained on a single
656 data set, it quickly reaches a good picking quality even when the training data only
657 contains few micrographs. Hence, increasing the size of the training data, enhances
658 the training time without benefitting the training. Therefore, only particles from 50
659 randomly selected micrographs and no more than 20,000 particles in total are used
660 for the training. Once the feedback loop is finalized, the picking performance is
661 further optimized by adjusting the picking threshold to an optimal one, as
662 determined by a parameter grid search using crYOLO's internal evaluation procedure.
663 The particle threshold value defines a confidence threshold that each pick made by
664 crYOLO must either meet or exceed in order to be accepted. If this threshold is set to
665 a low value, particles with a low confidence are also accepted. In order to find the
666 optimal threshold, a fixed subset of data is repeatedly picked while varying the
667 threshold from 0.0 to 1.0, using a step size of 0.01. Afterwards the optimal threshold

668 is defined by the highest F2 score ³¹ of all resulting picks. Processing results
669 generated with the optimized threshold are labeled with iteration "6 + T x.xxx",
670 where six represents the sixth and thus final model used in the feedback loop, and
671 the value x.xxx denotes the optimized picking threshold.

672 Picked particles are automatically extracted and classified in 2D, resulting in
673 class averages containing 60 to 100 particles per class (standard settings).
674 Classifications are performed by a new GPU-accelerated and updated version of
675 ISAC2, which is based on the original ISAC (Iterative Stable Alignment and Clustering)
676 algorithm¹⁹. Just like the CPU-bound ISAC2 it delivers high quality 2D class averages
677 as well as an initial clean-up of the data set, but does not come with the same high
678 computational cost. Hence, GPU ISAC provides the same functionality on a single
679 workstation without the need to outsource 2D classification to a cluster. The GPU
680 ISAC code repository is part of the SPHIRE repository listed above.

681 As the generation of high-resolution 2D class averages requires a sufficient number
682 of particles covering a range of views, 2D classification is only started once a certain
683 number of particles is accumulated. While this number can be adjusted in the
684 TransSPHIRE GUI, a default value of 20,000 particles per batch has proven to be good
685 (see also Supplementary Figure 4).

686 2D class averages are routinely used to assess the overall quality of the data
687 and to select only those particles for 3D refinement that contribute to high quality 2D
688 class averages. Previously, this selection was done manually, breaking any automated
689 processing pipeline. In order to provide a fully automated pipeline, TransSPHIRE uses
690 Cinderella ²⁰, a deep learning binary classifier based on a convolutional neural
691 network. When provided with a set of 2D class averages, Cinderella labels each of
692 them as either "good" or "bad." By default, this decision is based on a model that was
693 trained on a large set of class averages from a multitude of different cryo-EM

694 projects. Alternatively, Cinderella can be trained on specific data to select classes
695 according to the needs of the current project. By default, TranSPHIRE runs Cinderella
696 using its general model, based on 3,559 "good" and 2,433 "bad" classes taken from
697 20 different data sets from both the EMPIAR ³² data base and our in-house efforts.
698 The Cinderella git repository can be found online
699 (https://github.com/MPI-Dortmund/sphire_classes_autoselect).

700 Once the feedback loop has finished and a set of at least 200 "good" class
701 averages is available (number can be adjusted if desired), a reproducible, *ab initio* 3D
702 reconstruction is computed from 2D class averages using the SPHIRE method RVIPER
703 ¹³ (Reproducible Validation of Individual Parameter Reproducibility). The VIPER
704 algorithm combines a genetic algorithm ³³ with stochastic hill climbing ³⁴ to produce
705 multiple 3D ab initio structures. These reconstructions are then compared and the
706 most reproducible model is used to seed the consecutive 3D refinement. (See online
707 documentation for RVIPER and VIPER at
708 <http://sphire.mpg.de/wiki/doku.php?id=pipeline:viper:sxrviper>).

709 To generate a high-resolution 3D reconstruction a stack of all particles
710 assigned to classes that were labeled "good" by Cinderella is created. The
711 consecutive refinement is performed by the SPHIRE method MERIDIEN ¹³ providing
712 the initial reconstruction computed in the previous step as reference. The refinement
713 within MERIDIEN proceeds in two phases. The first phase, "EXHAUSTIVE", searches
714 the whole 3D parameter space -- three Euler angles for rotation and two dimensions
715 for translation -- on a discrete grid. The second phase, "RESTRICTED", searches the
716 parameter space on a discrete grid within the local area closest to the best matching
717 set of parameters found in the previous iteration. To avoid over-fitting, the image
718 dimensions and the grid spacing is adjusted after every iteration, based on the
719 achieved resolution according to the gold standard FSC ³⁵ and stability of the

720 parameters. In order to compensate for the discreteness of the grid and the
721 uncertainty in parameter assignment, particles are weighted by the probability of the
722 parameter set for the backprojection into the 3D reconstruction. (See online
723 documentation of MERIDIEN at
724 <http://sphire.mpg.de/wiki/doku.php?id=pipeline:meridien:sxmeridien>).

725 Similar to the prerequisites for 2D classification, a certain number of particles
726 representing different views is required to successfully compute a 3D reconstruction.
727 Thus, TranSPHIRE will not start the 3D refinement before a defined number of
728 particles is accumulated. In our hands a total of 40,000 particles (default value, can
729 be adjusted) is sufficient to calculate a medium to high resolution 3D reconstruction
730 in a short time frame. While this reconstruction will likely not reach the highest
731 resolution possible, it still enables a first analysis i.e. identification of a
732 conformational state or the verification if a ligand is bound or not. Furthermore, it
733 provides a quality control throughout the data acquisition, as a new 3D
734 reconstruction is computed for every batch of 40,000 particles. As all 3D refinements
735 start from the same initial reference, refinement projections parameters can
736 additionally be used to directly start with a local refinement of the complete data set,
737 thereby significantly reducing the required running time.

738

739 **Evaluation of the feedback performance**

740 As TranSPHIRE runs in parallel to the data acquisition and data are processed as they
741 come in, the number of movies is increasing during the runtime and results from one
742 feedback iteration to the next are not directly comparable. Thus, the feedback
743 performance was evaluated separately for every data set on a fixed subset of 500
744 (TRPC4 and Tc holotoxin, Figure 3-4) and 100 (Actomyosin, Figure 5) micrographs.

745 For each case, the fixed subset was processed using the intermediate picking models
746 produced during the individual feedback iterations. Specifically, every subset was
747 once picked with the starting model (general model, labeled round 1) and with every
748 picking model generated throughout the five iterations of the feedback loop (rounds
749 2 to 6) using a particle threshold of 0.1. In addition, another run was performed with
750 the final picking model using the optimized particle threshold (6 + T X.XX). The
751 consecutive processing in 2D and 3D was performed with AutoSPHIRE sp_auto.py,
752 which is the automatic, batch processing tool within SPHIRE ¹³ on our local CPU
753 cluster. The processing pipeline and settings used resemble the ones described
754 above, except that CPU ISAC was used instead of the new GPU-accelerated version.

755

756

757 **Automatic processing of the TRPC4 data.**

758 The performance of TranSPHIRE was tested on a subset of 500 micrographs of a high-
759 resolution data set of the transient receptor channel 4 (TRPC4) from zebra fish in
760 LMNG detergent (prepared in analogy to ³⁶, publication in preparation). The data set
761 was automatically collected at a Cs-corrected Titan Krios (FEI Thermo Fisher)
762 microscope equipped with an X-FEG and operated at 300kV using EPU (FEI Thermo
763 Fisher). Equally dosed frames with a pixel size of 0.85 Å/pixel were collected with a
764 K2 Summit (counting mode, Gatan) direct electron detector in combination with a
765 GIF quantum-energy filter set to a filter width of 20 eV. Each movie contains 50
766 frames and a total electron dose of 88.5 e/Å².

767 Processing in TranSPHIRE was performed as described above with five
768 internal feedback rounds to optimize the crYOLO picking model. Within the pipeline,
769 movies were drift corrected and dose weighted by MotionCor2 ¹⁴ using five patches
770 with an overlap of 20% and CTFFIND4 ¹⁶ fitted the CTF between 4 Å and 30 Å with an

771 Cs value of 0.001. The training data for the general model of crYOLO usually contain
772 four data sets of TRP channels. To avoid any favorable picking bias and handle the
773 TRPC4 data as previously unseen, the general model was retrained after removing all
774 TRP channels from the training data. Even then, crYOLO was able to identify most
775 TRPC4 particles through the successful generalization. To simulate a worst-case
776 scenario of a deficient initial picking performance, 90% of the particle picks in the
777 initial feedback round were replaced by random coordinates.

778 During the feedback rounds the crYOLO picking threshold was set to 0.1 and
779 the anchor size to the estimated particle diameter of 240 pixels. After the final
780 feedback round, the picking threshold value was adjusted to 0.257 based on the
781 crYOLO confidence threshold optimizing procedure described above. After each
782 particle picking step, particles were automatically extracted using SPHIRE
783 sp_window.py with a box size of 288 pixels. The subsequent 2D classification was
784 performed using a GPU accelerated version of the SPHIRE ISAC2 algorithm using
785 standard settings. The feedback loop was run with the default particle batch size of
786 20,000 (for details see above and Supplementary Figure 3).

787 The produced 2D class averages were subjected to an automatic 2D class
788 selection using our deep learning tool Cinderella and a confidence threshold of 0.1.
789 To simulate the processing of a previously unseen protein, Cinderella was trained
790 with its general model training data excluding all channel proteins, thereby ensuring
791 an unbiased selection process. During the feedback rounds crYOLO was trained on
792 the default value of 50 random micrographs that contained particles contributing to
793 classes labeled “good” by Cinderella. 3D reconstructions were computed as described
794 above using no mask and imposing c4 symmetry. Note that albeit our program
795 provides the possibility to compute a 3D mask from the initial model automatically
796 and apply it during the refinement, this option is deactivated by default. Automated

797 masking procedures might eliminate valid regions of the structure that are not well
798 resolved in the initial reconstruction, especially in cases with strong flexibility in the
799 complex. In case a 3D mask is not provided, we strongly recommend to use a mask
800 created from the results of TranSPHIRE for all follow-up experiments, in order to
801 exploit the full potential of 3D refinement. Whereas the workflow can be easily
802 extended, the pipeline for each batch stops by default after the first high resolution
803 3D refinement, in order to allow on-the-fly evaluation by the user. The results can be
804 easily converted to RELION after any milestone and *vice versa*. Correction of higher-
805 order aberrations for example in RELION might further improve the resolution of the
806 final result, when these optical effects are present³⁷.

807 The progression of the picking performance throughout the feedback rounds
808 was evaluated on a fixed subset of 500 micrographs as described above (Figure 3).
809 Note that the picking model of the first iteration is not included in this evaluation, as
810 its performance was initially corrupted by randomizing 90% of the picked particles.

811

812 **Automatic processing of the Tc holotoxin data.**

813 To test the capability of TranSPHIRE to target a specific conformation, a subset of 500
814 micrographs of the ABC holotoxin from *Photorhabdus Luminescens* reconstituted in a
815 lipid nanodisc (EMD-10313)²⁹ was processed. This data set contains a mixture of
816 conformations, namely the pre-pore and pore state of the holotoxin. The data set
817 was collected at a Cs-corrected Titan Krios (FEI Thermo Fisher) microscope equipped
818 with an X-FEG and operated at 300kV using EPU (FEI Thermo Fisher). Equally dosed
819 frames with a pixel size of 0.525 Å/pixel were collected with a K2 Summit (super
820 resolution mode, Gatan) direct electron detector in combination with a GIF quantum-
821 energy filter set to a filter width of 20 eV. Each movie contains 40 frames and a total
822 electron dose of 60.8 e/Å².

823 Processing in TranSPHIRE was performed as described above with five
824 internal feedback rounds to optimize the crYOLO picking model. Within the pipeline,
825 movies were drift corrected, dose weighted and binned to a pixel size of 1.05 Å/px by
826 MotionCor2 ¹⁴ using three patches without overlap and CTFFIND4 ¹⁶ fitted the CTF
827 between 4 Å and 30 Å with an Cs value of 0.001. Subsequently, particles were picked
828 using the general model of crYOLO.

829 During the feedback rounds the crYOLO picking threshold was set to 0.1 and the
830 anchor size to the estimated particle diameter of 205 pixels. After the final feedback
831 round, the picking threshold value was adjusted to 0.194 based on the crYOLO
832 confidence threshold optimizing procedure described above. After each particle
833 picking step, particles were automatically extracted using SPHIRE sp_window.py with
834 a box size of 420 pixels. The subsequent 2D classification was performed using a GPU
835 accelerated version of the SPHIRE ISAC2 algorithm using standard settings. The
836 feedback loop was run with the default particle batch size of 20,000 (for details see
837 above and Supplementary Figure 3).

838 The produced 2D class averages were subjected to an automatic 2D class
839 selection using our deep learning tool Cinderella and a confidence threshold of 0.1.
840 To demonstrate the ability of the TranSPHIRE feedback loop to selectively pick
841 particles of one conformational state, Cinderella was trained on pre-existing 2D class
842 averages of the pore state as instances of “good” classes (318) and 2D class averages
843 of the pre-pore state and contamination as instances of “bad” classes (664). During
844 the feedback rounds crYOLO was trained on the default value of 50 random
845 micrographs that contained particles contributing to classes labeled “good” by
846 Cinderella. 3D reconstructions were computed as described above without applying a
847 mask or symmetry.

848 The progression of the picking performance throughout the feedback rounds
849 was evaluated on a fixed subset of 500 micrographs as described above (Figure 4).

850

851 **Automatic processing of an actomyosin complex data set.**

852 A subset of 100 micrographs of an actomyosin complex with a bound small molecule
853 ligand (publication in preparation) was chosen to demonstrate the processing of
854 filamentous samples and within TranSPHIRE and its suitability for high-throughput
855 ligand screenings. The data set was collected at a Cs-corrected Titan Krios (FEI
856 Thermo Fisher) microscope equipped with an X-FEG and operated at 300kV using
857 EPU (FEI Thermo Fisher). Equally dosed frames with a pixel size of 0.56 Å/pixel were
858 collected with a K2 Summit (super resolution mode, Gatan) direct electron detector
859 in combination with a GIF quantum-energy filter set to a filter width of 20 eV. Each
860 movie contains 40 frames and a total electron dose of 81.2 e/Å².

861 Processing in TranSPHIRE was performed as described above with five internal
862 feedback rounds to optimize the crYOLO picking model. Within the pipeline, movies
863 were drift corrected, dose weighted and binned to a pixel size of 1.10 Å/px by
864 MotionCor2¹⁴ deactivating patch alignment and CTFFIND4¹⁶ fitted the CTF between
865 5 Å and 30 Å with an Cs value of 0.001.

866 As the crYOLO general model does not include filamentous data it cannot be
867 readily applied to this data set. Instead a new crYOLO general model specific for actin
868 filaments was trained. The training data consisted of multiple actin data sets
869 collected within our group, but did not include any data of an actomyosin complex or
870 other actin complexes. Considering the significant optical difference of actin and
871 actomyosin filaments (also see Figure 5), picking with the general actin crYOLO model
872 mimics the processing of a previously unseen filamentous protein.

873 During the feedback rounds the crYOLO picking threshold was set to 0.1 and
874 the anchor size to the estimated box size of 320 pixels. Furthermore, the filament
875 width was set to 100 px and the box distance to 25 px (equivalent to one helical rise
876 of 27.5 Å). Only filaments consisting of at least six segments were considered. After
877 the final feedback round, the picking threshold value was adjusted to the crYOLO
878 default value of 0.3, as the threshold optimization procedure of crYOLO does not
879 support filaments. After each particle picking step, particles were automatically
880 extracted using SPHIRE sp_window.py with a box size of 320 pixels and a filament
881 width of 100 pixels. The subsequent 2D classification was performed using a GPU
882 accelerated version of the SPHIRE ISAC2 algorithm asking for 30-50 particles per
883 class. The feedback loop was run with the default particle batch size of 20,000 (for
884 details see above and Supplementary Figure 3).

885 The produced 2D class averages were subjected to an automatic 2D class
886 selection using our deep learning tool Cinderella and a confidence threshold of 0.1.
887 As filamentous data differ strongly from the data used to train the general model of
888 Cinderella, a new model was trained based on the 2D class averages produced in the
889 initial feedback round combined with previously selected class averages of actin only
890 data sets. During the feedback rounds crYOLO was trained on the default value of 50
891 random micrographs that contained particles contributing to classes labeled “good”
892 by Cinderella.

893 An initial 3D reference was created from a deposited actomyosin atomic
894 model (PDB:5JLH)³⁸. The 3D refinement was performed using SPHIRE
895 sp_meridien_alpha.py, an open alpha version of helical processing in SPHIRE, with a
896 particle radius of 144 px (~45% of the box size), a filament width of 100 px and a
897 helical rise of 27.5 Å. While projection parameters are restrained according to the
898 helical parameters e.g. the shift along the filament axis is restricted to half of the rise,

899 no helical symmetry is applied and therefore does not need to be determined
900 beforehand. To avoid artifacts due to the contact of the filament to the edges of the
901 box, a soft 3D mask covering 85% percent of the filament was applied during the
902 refinement.

903 The progression of the picking performance throughout the feedback rounds was
904 evaluated on a fixed subset of 100 micrographs as described above (Figure 5).

905

906 **Acknowledgements**

907 The authors thank T. Shaik for carefully reading the manuscript and valuable
908 comments, and O. Hofnagel and D. Prumboam for testing and their continuous
909 feedback. We further thank D. Roderer and D. Vinayagam for providing the TRPC4
910 and Tc holotoxin data sets, respectively. This work has been funded by the Max
911 Planck Society (S.R.).

912

913 **Author contributions**

914 **Conceptualization:** M.S., T.W., C.G. and S.R.;

915 **Software - TranSPHIRE:** M.S.;

916 **Software - GPU ISAC:** F.S.;

917 **Software - Cinderella:** T.W.;

918 **Formal Analysis:** M.S., T.W., S.P.;

919 **Writing – Original Draft:** F.S.;

920 **Writing – Review & Editing:** F.S., M.S., S.P., T.W., C.G., S.R.;

921 **Funding Acquisition:** S.R.

922

923

924 **Competing interests**

925 The authors declare no competing interests.

926

927 **Data availability**

928 The movies processed in this manuscript are subsets of data sets that are published
929 (Tc holotoxin ²⁹) or will be published elsewhere (TRPC4 and actomyosin) and are
930 available from the corresponding author upon reasonable request.

931

932 **Code availability**

933 TransPHIRE is open-source and can be downloaded free of charge
934 (<https://github.com/MPI-Dortmund/transphire>).

935

936 **References**

- 937 1. Nogales, E. The development of cryo-EM into a mainstream structural biology
938 technique. *Nat. Methods* **13**, 24–27 (2016).
- 939 2. Method of the Year 2015. *Nature Publishing Group* 1–1 (2015).
940 doi:10.1038/nmeth.3730
- 941 3. Merino, F. & Raunser, S. Cryo-EM as a tool for structure-based drug
942 development. *Angewandte Chemie* (2016). doi:10.1002/ange.201608432
- 943 4. Schenk, A. D., Cavadini, S., Thomä, N. H. & Genoud, C. Live Analysis and
944 Reconstruction of Single-Particle Cryo-Electron Microscopy Data with
945 CryoFLARE. *J Chem Inf Model* *acs.jcim.9b01102* (2020).
946 doi:10.1021/acs.jcim.9b01102
- 947 5. Zivanov, J. *et al.* New tools for automated high-resolution cryo-EM structure
948 determination in RELION-3. *Elife* **7**, (2018).

949 6. Tegunov, D. & Cramer, P. Real-time cryo-electron microscopy data
950 preprocessing with Warp. *Nat. Methods* **16**, 1146–1152 (2019).

951 7. Maluenda, D. *et al.* Flexible workflows for on-the-fly electron-microscopy
952 single-particle image processing using Scipion. *Acta Crystallogr D Struct Biol*
953 **75**, 882–894 (2019).

954 8. Biyani, N. *et al.* Focus: The interface between data collection and data
955 processing in cryo-EM. *J. Struct. Biol.* **198**, 124–133 (2017).

956 9. Punjani, A., Rubinstein, J. L., Fleet, D. J. & Brubaker, M. A. cryoSPARC:
957 algorithms for rapid unsupervised cryo-EM structure determination. *Nat.*
958 *Methods* (2017). doi:10.1038/nmeth.4169

959 10. Lander, G. C. *et al.* Appion: an integrated, database-driven pipeline to
960 facilitate EM image processing. *J. Struct. Biol.* **166**, 95–102 (2009).

961 11. Suloway, C. *et al.* Automated molecular microscopy: the new Leginon system.
962 *J. Struct. Biol.* **151**, 41–60 (2005).

963 12. Wagner, T. *et al.* SPHIRE-crYOLO is a fast and accurate fully automated particle
964 picker for cryo-EM. *Commun Biol* **2**, 218 (2019).

965 13. Moriya, T. *et al.* High-resolution Single Particle Analysis from Electron Cryo-
966 microscopy Images Using SPHIRE. *J Vis Exp* e55448–e55448 (2017).
967 doi:10.3791/55448

968 14. Zheng, S. Q. *et al.* MotionCor2: anisotropic correction of beam-induced
969 motion for improved cryo-electron microscopy. *Nat. Methods* (2017).
970 doi:10.1038/nmeth.4193

971 15. Grant, T. & Grigorieff, N. Measuring the optimal exposure for single particle
972 cryo-EM using a 2.6 Å reconstruction of rotavirus VP6. *Elife* **4**, e06980 (2015).

973 16. Rohou, A. & Grigorieff, N. CTFFIND4: Fast and accurate defocus estimation
974 from electron micrographs. *J. Struct. Biol.* **192**, 216–221 (2015).

975 17. Penczek, P. A. *et al.* CTER-rapid estimation of CTF parameters with error
976 assessment. *Ultramicroscopy* **140**, 9–19 (2014).

977 18. Zhang, K. Gctf: Real-time CTF determination and correction. *J. Struct. Biol.*
978 **193**, 1–12 (2016).

979 19. Yang, Z., Fang, J., Chittuluru, J., Asturias, F. J. & Penczek, P. A. Iterative stable
980 alignment and clustering of 2D transmission electron microscope images.
981 *Structure* **20**, 237–247 (2012).

982 20. Wagner, T. Cinderella. (2019). doi:10.5281/zenodo.3672421

983 21. Hohn, M. *et al.* SPARX, a new environment for Cryo-EM image processing. *J.*
984 *Struct. Biol.* **157**, 47–55 (2007).

985 22. Bepler, T. *et al.* Positive-unlabeled convolutional neural networks for particle
986 picking in cryo-electron micrographs. *Nat. Methods* **16**, 1153–1160 (2019).

987 23. Wang, F. *et al.* DeepPicker: A deep learning approach for fully automated
988 particle picking in cryo-EM. *J. Struct. Biol.* **195**, 325–336 (2016).

989 24. Behrmann, E. *et al.* Real-space processing of helical filaments in SPARX. *J.*
990 *Struct. Biol.* **177**, 302–313 (2012).

991 25. He, S. & Scheres, S. Helical reconstruction in RELION. 1–27 (2016).
992 doi:10.1101/095034

993 26. Rohou, A. & Grigorieff, N. Frealign: model-based refinement of helical filament
994 structures from electron micrographs. *J. Struct. Biol.* **186**, 234–244 (2014).

995 27. Egelman, E. H. The iterative helical real space reconstruction method:
996 surmounting the problems posed by real polymers. *J. Struct. Biol.* **157**, 83–94
997 (2007).

998 28. Wagner, T. *et al.* Two particle picking procedures for filamentous proteins:
999 SPHIRE-crYOLO filament mode and SPHIRE-STRIPER. **2**, 218–23 (2020).

1000 29. Roderer, D., Hofnagel, O., Benz, R. & Raunser, S. Structure of a Tc holotoxin
1001 pore provides insights into the translocation mechanism. *Proc. Natl. Acad. Sci.*
1002 *U.S.A.* **116**, 23083–23090 (2019).

1003 30. Kremer, J. R., Mastronarde, D. N. & McIntosh, J. R. Computer visualization of
1004 three-dimensional image data using IMOD. *J. Struct. Biol.* **116**, 71–76 (1996).

1005 31. Sokolova, M. & Lapalme, G. A systematic analysis of performance measures
1006 for classification tasks. *Information Processing and Management* **45**, 427–437
1007 (2009).

1008 32. Iudin, A., Korir, P. K., Salavert-Torres, J., Kleywelt, G. J. & Patwardhan, A.
1009 EMPIAR: a public archive for raw electron microscopy image data. *Nat.*
1010 *Methods* **13**, 387–388 (2016).

1011 33. Mirjalili, S., Song Dong, J., Sadiq, A. S. & Faris, H. in *Nature-Inspired*
1012 *Optimizers: Theories, Literature Reviews and Applications* (eds. Mirjalili, S.,
1013 Song Dong, J. & Lewis, A.) 69–85 (Springer International Publishing, 2020).

1014 34. Elmlund, H., Elmlund, D. & Bengio, S. PRIME: probabilistic initial 3D model
1015 generation for single-particle cryo-electron microscopy. *Structure* **21**, 1299–
1016 1306 (2013).

1017 35. Henderson, R. *et al.* Outcome of the first electron microscopy validation task
1018 force meeting. in **20**, 205–214 (2012).

1019 36. Vinayagam, D. *et al.* Electron cryo-microscopy structure of the canonical
1020 TRPC4 ion channel. *Elife* **7**, 213 (2018).

1021 37. Zivanov, J., Nakane, T. & Scheres, S. H. W. Estimation of high-order
1022 aberrations and anisotropic magnification from cryo-EM data sets in RELION-
1023 3.1. *IUCrJ* **7**, 253–267 (2020).

1024 38. Ecken, von der, J., Heissler, S. M., Pathan-Chhatbar, S., Manstein, D. J. &
1025 Raunser, S. Cryo-EM structure of a human cytoplasmic actomyosin complex at
1026 near-atomic resolution. *Nature* **534**, 724–728 (2016).

1027